

## Article

# Laboratory and Full-Scale Testbed Study in the Feasibility of Styrene-Butadiene-Styrene Asphalt Pavement Having Epoxy Resin and Crumb Rubber Powder

Sang-Yum Lee <sup>1</sup>  and Tri Ho Minh Le <sup>2,\*</sup><sup>1</sup> Faculty of Civil Engineering, Induk University, 12 Choansan-ro, Nowon-gu, Seoul 01878, Republic of Korea<sup>2</sup> Faculty of Civil Engineering, Nguyen Tat Thanh University, 300A Nguyen Tat Thanh Street, District 4, Ho Chi Minh City 70000, Vietnam

\* Correspondence: lhmtri@ntt.edu.vn

**Abstract:** Conventional asphalt concrete pavements have deteriorated rapidly due to the current increased traffic and extreme climate impacts. In addition to the upgrading in the construction quality, there is an urgent need to expand the utilization of modified asphalt binders to improve road capacity and traffic safety. The proposed research aims to combine epoxy resin (ER) and crumb rubber powder (CRP) contents into conventional Styrene-butadiene-styrene (SBS)-modified asphalt binder to not only reduce the consumption of normal asphalt binder but also promote the usage of recycled waste material in practice. To cope with this research objective, the ER and CRP were designed at 3% and 5% by weight of asphalt binder, respectively. Various laboratory tests were performed to evaluate the performance of modified mixtures (ERCRP), including the Frequency Sweep Test, Multiple Stressed Creep and Recovery, Dynamic Modulus, Semi-Circular Bending (SCB), and Cantabro Durability Tests. Additionally, an assessment of the modified asphalt concrete pavement via field testbed was conducted through Falling Weight Deflectometer and Ground Penetrating Radar. Overall, by adding the ER and CRP, the strain value of the control reference mix can be reduced up to 31.8% and 28.3% at MSCR 0.1 and 3.1 kPa, respectively. Additionally, the dynamic modulus of the ERCRP-modified samples was approximately 32,267 and 189 MPa, while the value of the reference mixture was 28,730 and 105 MPa at the highest and lowest frequency, respectively, indicating an enhancement under repeated loads. Regarding the SCB test results at 0 °C, the peak stress of the ERCRP-modified mixture was 4.75 MPa, while the value of the reference specimens was only 4.2 MPa, noticing the improved stress-bearing capacity. Based on a full-scale testbed, the FLWD elastic modulus of reinforced pavement shows a novel improvement (6.75%) compared with the control pavement, suggesting a potential application of ERCRP-modified asphalt binder for sustainable development purposes.

**Keywords:** sustainable development; full-scale testbed; modifier asphalt binder; crumb rubber powder; epoxy resin; SBS asphalt pavement



**Citation:** Lee, S.-Y.; Le, T.H.M. Laboratory and Full-Scale Testbed Study in the Feasibility of Styrene-Butadiene-Styrene Asphalt Pavement Having Epoxy Resin and Crumb Rubber Powder. *Buildings* **2023**, *13*, 652. <https://doi.org/10.3390/buildings13030652>

Academic Editors: Andrea Baliello and Di Wang

Received: 8 February 2023

Revised: 27 February 2023

Accepted: 27 February 2023

Published: 28 February 2023



**Copyright:** © 2023 by the authors. Licensee MDPI, Basel, Switzerland. This article is an open access article distributed under the terms and conditions of the Creative Commons Attribution (CC BY) license (<https://creativecommons.org/licenses/by/4.0/>).

## 1. Introduction

Over the past decades, the physical properties of road pavement have rapidly deteriorated due to increased traffic and environmental impacts [1,2]. Multiple strategies have been proposed to increase road capacity as well as traffic safety. In addition to the enhancement in construction technologies, the modification of asphalt binders has gained attention recently since this coating material can greatly contribute to the durability and workability of the binder [3]. To cope with this objective, synthetic polymers have been developed to represent the efficiency modifiers in asphalt binders [4]. These materials are often mixed into the asphalt at a weight ratio of 3–8% to improve the physical properties of the asphalt that is used in road pavement [5]. Modified asphalt properties have been altered to improve pavement resistance to damage, such as plastic deformation and

thermal cracking [6]. Asphalt modifiers can provide improved resistance performance to the aforementioned damage by mixing the modifier into the asphalt during production (wet-mix) and dry mix type, which introduces the modifier together with the asphalt when producing the HMA (Hot Mix Asphalt) [5].

Asphalt modification that uses polymers is intended to reduce pavement damage, improve road durability, and reduce road management costs. However, not all polymers can be used as asphalt modifiers [7]. The most important requirement is that the polymer has compatibility with asphalt [6]. Therefore, when the polymer is mixed with the asphalt, it should exhibit a single phase without phase separation. In general, if two materials have similar structures or similar polarity, they mix well with each other and become a single-phase mixture [8]. Compatibility equates to storage ability, and it indicates stability. Here, the polymer becomes swollen as it is partially surrounded by maltene, an oily aromatic compound of asphalt.

Polymers that are used as modifiers are divided into three types. They are thermoplastic elastomers, thermoplastics, and reactive polymers. The most typical thermoplastic elastomer (TPE) is the styrene-butadiene-styrene triblock copolymer (SBS), and another typical TPE is the styrene-isoprene (2-methyl butadiene)-styrene triblock copolymer (SIS) which is similar to SBS [9]. These have a biphasic structure in which a crystallized styrene portion is connected to an amorphous butadiene region and overall, it forms a network structure [10]. When these polymers are mixed with asphalt by heat and shear force, the butadiene portion swells due to the asphalt's maltene, and the modified asphalt retains this network structure even when it cools [10]. Therefore, the characteristic elasticity of these polymers is transferred to the modified asphalt, and the asphalt exhibits excellent elastic recovery and permanent deformation resistance [11]. However, these modification methods have two main disadvantages. One is that solid rubber must be dissolved by heat in order to mix the rubber polymers with the asphalt. To do this, high heat is required for a long period of time, and a strong shear force is required during mixing because the dissolved rubber is highly viscous, and this leads to high costs [10,12]. The other disadvantage is the C=C double bond that exists in butadiene. The double bond is vulnerable to heat and oxygen in the air and is easily broken, which reduces the durability of the modified asphalt.

The second type of polymer that is used as a modifier is thermoplastic. PE (polyethylene) and EVA (ethylene-vinyl acetate copolymer) are typical thermoplastics [13]. The advantage of these polymers is that they are easy to purchase and low-cost, and they are particularly environmentally friendly because recycled products can be used. In the case of these modifiers, the high stiffness and deformation resistance that is characteristic of plastic polymers is transferred to the asphalt [3]. However, because PE is highly crystalline, non-polar, and amorphous, it does not mix well with asphalt, which is polar. Therefore, it will float to the top of the asphalt if left alone due to its difference in density ( $0.94 \text{ g/cm}^3$ ) [13]. This reduces the storage stability of the modified asphalt [14]. To make it mix well with asphalt, an acetate group ( $\text{CH}_3\text{COO}$ ) is used to reduce crystallinity, an ester group is used to increase polarity slightly, and the result is EVA [15].

The third type of polymer that is used as a modifier is a reactive polymer. Elvaloy and Lotader are typical reactive polymers. These are ethylene-butyl acrylate-glycidyl methacrylate terpolymers, and their polarity is increased by the acrylic group [16]. Furthermore, the glycidyl group ( $\text{CH}_2\text{OCH}_2\text{-CH}_2\text{-}$ ) reacts with the carboxyl group to form a covalent bond so that they mix well with asphalt [17]. However, this reaction creates an asphalt gel and prevents the formation of a network structure in the modified asphalt. Therefore, these polymers are not suitable as asphalt modifiers, and in practice, they are mainly used as adhesives in the plastics industry [18].

Recent studies have estimated that 2 billion tires are disposed of worldwide each year [19]. This accounts for two to three percent of the entire volume of industrial waste. Sales of vehicles are rising along with the world's population, especially in developing countries with more accessibility to vehicles [8]. Further, additional tires must be replaced after prolonged exposure to commuting increases the volume of discarded tires [20]. As

a result, the rapid increase in the number of discarded tires imposes a significant hazard to the environment. Despite resource conservation efforts and government controls, tires continue to be treated improperly. Once they are stored in landfills, tires tend to leach contaminants into the atmosphere, ground, and water, which can cause environmental disruption. Carbon dioxide can be released into the air when used tires are subjected to the sun. This carbon dioxide causes an increase in air pollution, which could cause climate change as well [20].

The utilization of used tires in practical application is proven to be an increasingly viable remedy to the problem [21]. Although only a minimal amount of waste tires is reclaimed each year, recycling waste tires has emerged as the primary method for the handling of this material in the EU, where it represents about 40 percent of the total of all waste tires. As a result, the consumption of recycled tires would considerably enhance the goals of green construction in the world. As a viable reinforced component in the asphalt pavement industry, discarded tire rubber powder has been utilized as a vital additive for hot asphalt mixtures [21]. The benefits of Crumb Rubber Powder (CRP) asphalt include decreased contamination issues, stronger bearing capacity, and resilience to permanent distortion. In contrast to conventional bitumen, CRP asphalt has increased viscosity in hot regions and reduced rigidity in cold areas [22]. Reduced rigidity at low temperatures can contribute to the high capacity to prevent thermal cracking, while the high viscosity property can provide excellent resilience to rutting imposed by transportation volume.

Although various researchers have examined the application of modifiers in asphalt binder, there is a lack of research investigating the combined effect of epoxy resin and crumb rubber powder in SBS-modified asphalt. The full-scale applicability of the SBS-modified asphalt using both ER and CRP also shows limited findings. Therefore, the proposed research aims to determine the adaptability of mixing ER and CRP into polymer-modified asphalt in both laboratory and full-scale testbed experiments to promote the consumption of by-product material in practice as well as ensure the durability of the conventional pavement structure. Regarding the mix design overview, the CRP and ER were substituted 5% and 3% by weight of SBS-modified asphalt binder, respectively. Afterward, the proposed research employed a variety of testing methods to evaluate the physical properties of modified asphalt containing the Frequency Sweep Test, Multiple Stressed Creep and Recovery, Dynamic Modulus, Semi Circular Bending, and Cantabro Durability Tests. Further, a long-term performance investigation in the field testbed was also conducted by using Falling Weight Deflectometer and Ground Penetrating Radar. In the evaluations, conventional modified asphalts were used for a comparative evaluation of the developed material. The general summary of the research is presented in Figure 1.

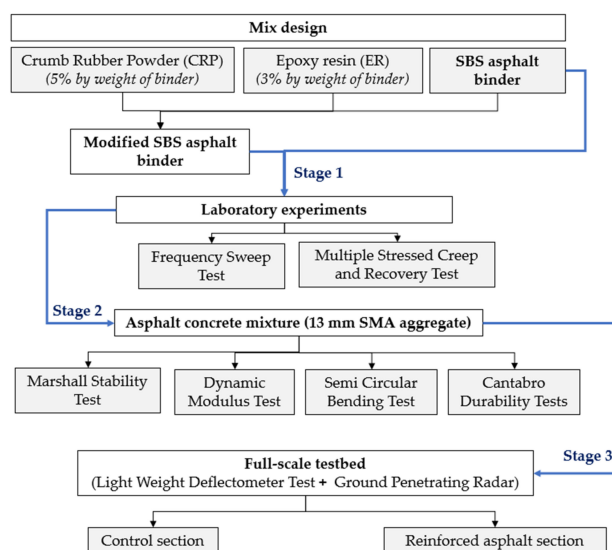


Figure 1. Research flowchart.

## 2. Materials and Methods

### 2.1. Aggregates and Asphalt Binder

#### 2.1.1. Aggregates

The aggregate and fillers for this research were provided by a Korean Company, and the basic properties of the material are shown in Table 1. Following previous studies and suggestions of relevant studies, the ideal asphalt binder constitutes 5–6% of the total weight [17,18], and this work developed samples using the Superpave technique. The goal of Superpave was to propose a technique that would maximize the asphalt mixture's durability against rutting, fatigue cracking, and thermal cracking while making the optimum utilization of bitumen pavement methods. The Superpave Gyrotory Compactor (SGC) determines the volumetric and compression qualities of the materials, and the data collected by the SGC throughout compression can be used to generate insight into the workability of the specific combination [23].

**Table 1.** Aggregate and mineral filler properties.

Materials	Properties	Value
Aggregate	Relative apparent density [24]	2.73
	Water absorption [24]	0.182%
	Aggregate crushed value [25]	17.7%
	Los Angeles abrasion value [26]	25.8%
	Flakiness and elongation index [27]	12.8%
Mineral Filler	Relative apparent density [28]	2.31
	Moisture content [28]	0.08%

The development of a polymer-modified asphalt binder mixture (PG 76-22) was performed using a 13 mm SMA aggregate type. Since the stress from the vehicle load is borne entirely by the aggregate in the stone mastic asphalt (SMA), the usage of this aggregate type can counter the binder delamination (desorption) based on the adhesive force between the aggregate [29] in the conventional asphalt mixture. The synthetic particle sizes distribution of the aggregate that was created in this test is summarized in the following Table 2.

**Table 2.** Mix design for 13 mm SMA mixture design particle size table.

Sieve size	Corrected Mixing Ratio (%)				
	Synthesis Rate (%)				
	14–20 mm	11–14 mm	7–11 mm	Fine Aggregate	Filler
	-	59.0	17.0	13.0	11.0
25 mm	-	-	-	-	-
20 mm	-	100.0	100.0	100.0	100.0
13 mm	-	96.4	100.0	100.0	100.0
10 mm	-	18.3	97.6	100.0	100.0
5 mm	-	1.3	1.7	95.1	100.0
2.5 mm	-	0.6	0.7	69.5	100.0
0.6 mm	-	0.1	0.1	37.5	100.0
>0.3 mm	-	0.0	0.0	27.7	97.2
0.15 mm				18.8	92.2
0.08 mm				10.0	73.0

### 2.1.2. Asphalt Binder

Styrene-butadiene-styrene (SBS) was employed to strengthen the primary asphalt binders utilized in the proposed approach. SBS is well recognized for being flexible in ambient conditions and having the capability to boost a binder's elasticity. This SBS compound can increase the performance of a mixture and the applicability of bitumen by lowering the mixing energy and the stiffness of asphalt.

Regarding the epoxy resin, bisphenol A diglycidyl ether was employed as the epoxy resin in this research. The accompanied curing agents were also provided by the equivalent Korean chemical company. The ER has the Epoxy Equivalent (g/mol) of 193, while the unhydrolytic chlorine (%) and hydrolyzable chlorine (%) were 0.011 and 0.1, respectively. The epoxy solution to curing ingredient mass distribution is 100:65 based on [30].

As for the CRP, it was produced via a mechanochemical process with enabled CRP having a particle diameter of 30 mesh. A synthetic ingredient (organic disulfide) was applied using mechanical power to speed up the reaction process [31]. Regarding the previous investigation, the activated technique conditions of the mechanochemical method that uses the organic disulfide ingredient (5% of CRP by wt.) were modified [32]. According to the preliminary experimental results, blending SBS and CRP produces a substance with very low workability. Accordingly, in order to produce a uniform solution and achieve the desired air void ratio, the heat of the production processes was tightly regulated. Based on the trial works, the combining procedure was controlled at 165 °C for 40 min using a 3% organic disulfide content.

### 2.1.3. Mixture Design

Following the mixing process, the normal SBS asphalt binder was conditioned at 165 °C for one hour to a melted condition before adding ER and CRP. SBS asphalt binder was blended with CRP and ER; then the mixture was stirred for 5 min at a speed of 1000 rpm. To achieve a homogeneous combination of the SBS-ER-CRP, the curing agent was introduced to the aforementioned combination and swirled for an additional 5 min at a rate of 1500 rpm. The fundamental characteristics of asphalt binders treated with ERCRP are presented in Table 3, and the general test results of the ERCRP mixture are shown in Table 4.

**Table 3.** Properties of asphalt binder.

Properties	Value
Penetration (1/10 mm) 25 °C [33]	85.8
Softening point (°C) [34]	68.7
Ductility at 5 °C (cm/min) [35]	99.3
$G^*/\sin\delta$ ; (Original) [36]	1.71 kPa
$G^*/\sin\delta$ (after RTFO) [36]	2.43 kPa
$G^* \times \sin\delta$ (after PAV) [37]	1501 kPa
Stiffness [38]	182 MPa
m-value [38]	0.32

**Table 4.** General property test results of the modified mixture.

	Asphalt Content (%)	Porosity (%)	Saturation (%)	Marshall Stability (N)	Flow Value(1/100)	Aggregate Porosity (%)	Effective Density	Theoretical Maximum Density (g/cm <sup>3</sup> )
Standard	-	3~6	65~80	>7500	20~40	>13		
Average	5.3%	3.8	75.5	12,773	37.4	15.36	2.710	2.508

## 2.2. Binder Tests

### 2.2.1. Frequency Sweep Test

The Frequency Sweep Test (FST) is a very convenient test that can evaluate the rheological properties of a viscoelastic material according to time and temperature, and it is useful for checking the basic behavior of binders over a wide range of temperatures. In this study, FST was performed on the polymer-modified asphalt and the control mixture to create a master curve of the dynamic shear modulus, which can be used to predict the behavior of binders. The dynamic shear master curve can be used to compare the physical properties of asphalt binders, and it can be used as basic data for estimating the physical properties of asphalt mixtures in the future [39].

In this study, FST was conducted based on a dynamic shear rheometer based on ASTM D7552-22 [40]. Dynamic shear tests that use a dynamic shear rheometer (DSR) are generally used to analyze the viscous and elastic behavior characteristics of the asphalt binder that is in use, and it is possible to understand the physical property changes in the asphalt at the pavement's usage temperature by measuring the complex shear modulus ( $G^*$ ) and the phase angle ( $\delta$ ) [41]. Methods for analyzing the rheological properties of asphalt using a DSR include the temperature sweep test (TST), which measures rheological behavior properties according to temperature, and the strain sweep test (SST), which measures the linear viscoelastic region of the asphalt and selects a strain rate [42]. These tests were performed at a strain level of 1.0% which was determined by the SST to create a master curve of the dynamic shear modulus, and tests were performed at 12 temperatures at 7 °C intervals from 13 °C to 90 °C to obtain the dynamic shear modulus for a wide range of temperatures. In the frequency sweep test, this research follows the popular standards as shown in related research [43,44]. Additionally, the number of testing temperatures was increased compared with the conventional method to better develop the dynamic shear modulus and quantify the behavior of the modified binder under various testing temperatures. As for the size of the binder specimen, a specimen with a thickness of 2 mm and a diameter of 8 mm was used at 48 °C and below, and a specimen with a thickness of 1 mm and a diameter of 25 mm was used at 48 °C and above to reduce error following ASTM standards [40]. The tests used a load control test method that repeatedly applies loads at varying frequencies within multiple temperature ranges, and the loading frequencies are outlined in Table 5.

**Table 5.** Each load cycle (Time Temperature Superposition).

Angular Frequency (rad/s)					
6.28	9.96	15.75	25.01	39.64	62.83

### 2.2.2. Multiple Stressed Creep and Recovery (MSCR) Test

The MSCR test is a testing method that was recently presented in ASTM D7405-10a [45] and AASHTO TP70 [46] for evaluating the high-temperature elastic recovery of asphalt binders, and it is mainly used to evaluate the high-temperature elastic recovery of asphalt binders. The existing ASTM D6373 [47] binder selection method recommends using a binder grade that is one or two steps above the grade determined by DSR tests if there is a high traffic volume or a low vehicle traveling speed in the area where the binder will be used. However, this method has a problem since it may lead to the use of unnecessary high-cost modified binders because this approach is used indiscriminately even when the area's maximum temperature is relatively low.

The MSCR test has the advantage of adequately reflecting the elastic and viscoelastic properties for evaluating the plastic resistance of asphalt binders by considering material properties in a relatively large strain rate range, and it performs evaluations after simulating the stress conditions that the mixture may experience due to the actual load. The loads that were used in MSCR were 0.1 kPa and 3.2 kPa, as suggested by ASTM D7405-10a [45] and AASHTO TP70 [46]. The 0.1 KPA load was applied for 1 s followed by a 9-s rest, and this

process was repeated 10 times. Then, the load was increased to 3.2 kPa, and the process was repeated in the same way. Table 6 summarizes the load conditions that include the 2 load levels suggested by ASTM D7405-10a and AASHTO TP70, respectively. Figure 2 shows the stress curve and the resulting strain rate curve when loads of a certain size were applied and then a rest period was allowed. Figure 2A shows the applied shear stress, and Figure 2B shows the recoverable viscoelastic strain rate and the non-recoverable plastic deformation ( $\epsilon_{\text{recoverable}}$  and  $\epsilon_{\text{irrecoverable}}$ ) that can occur due to shear stress, respectively [39].

Table 6. MSCR test process.

Number of Loads	1	2	3	4	5	6	7	8	9	10
Creep (kPa)	0.1	0.2	0.4	0.8	1.6	3.2	6.4	12.8	25.6	61.2
Time and Repetition	<ul style="list-style-type: none"> <li>■ Creep load time (seconds) = 1.0</li> <li>■ Recovery time (seconds) = 9.0</li> <li>■ Number of creep and recovery iterations = 10</li> </ul>									

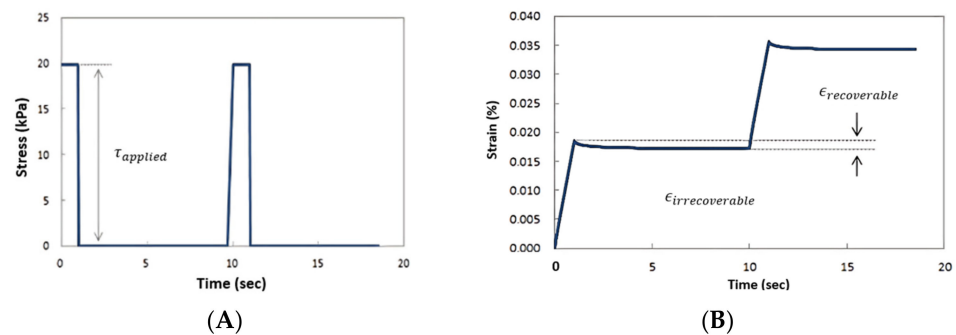


Figure 2. (A) Example of stress curve of MSCR test; (B) Example of strain curve of MSCR test.

The MSCR test applies loads of a fixed level on specimens and then allows them for rest periods. The non-recoverable compliance  $J_{\text{nr}}$  can be obtained by dividing the unrecovered plastic strain rate by the level of the applied shear load, as shown in Equation (1) below. Generally, as the level of the load increases, the  $J_{\text{nr}}$  value increases, and at the same load,  $J_{\text{nr}}$  tends to increase as the binder's plastic deformation resistance decreases. Therefore, the maximum value of  $J_{\text{nr}}$  is suggested as the evaluation standard for the binder, as shown in the following Equation [45].

$$J_{\text{nr}} = \frac{\epsilon_{\text{irrecoverable}}}{\tau_{\text{applied}}} \quad (1)$$

where  $J_{\text{nr}}$  is the non-recoverable compliance,  $\epsilon_{\text{irrecoverable}}$  is the non-recoverable shear strain rate, and  $\tau_{\text{applied}}$  is the shear load.

In addition, the recoverable strain rate and the non-recoverable strain rate defined in the equation above can be used to determine the recovery percentage that is shown in Equation (2) below [45]. This can be used to effectively distinguish the elastic recovery properties of two different binders in which the same maximum strain rate occurs at the same load, and it can be used to effectively evaluate the properties of modified binders.

$$\text{Recovery}(\%) = \frac{\epsilon_{\text{recoverable}}}{\epsilon_{\text{peak}}} \quad (2)$$

where, recovery (%) is the recovery rate;  $\epsilon_{\text{recoverable}}$  is the recoverable shear strain rate;  $\epsilon_{\text{peak}}$  is the maximum shear strain rate.

### 2.3. Asphalt Concrete Mixture Tests

#### 2.3.1. Dynamic Modulus Test

The dynamic modulus can depict a variety of traffic conditions using various temperature conditions, loads, and speeds, and it changes according to the asphalt binder and the particle size of the aggregate that is used. It can be considered to be a physical property evaluation method that can depict the viscoelastic properties of asphalt mixtures particularly well. The viscoelastic behavior properties of asphalt mixtures can be identified based on the correlation between the deformation properties and the load that is measured when a sine-wave load is applied continuously without a rest period, and the parameter that is used here can be defined as the complex modulus ( $E^*$ ). The dynamic modulus values that are determined by the tests can be obtained based on the combination of test temperature and load. The master curve of the dynamic modulus and the transition function was calculated by using the superposition principle for the previously mentioned load time and temperature to the dynamic modulus values. The method that is recommended by AASHTO TP 62 [48] uses the viscosity properties of the asphalt binder, and it is called the viscosity-temperature susceptibility method. It uses the slope of the viscosity value according to the changes in the absolute temperature on a logarithmic graph. The relationship between viscosity and temperature susceptibility can be expressed in Equation (3) below [49].

$$\log(\log \eta) = A + VTS[\log(T_R)] \quad (3)$$

Here,  $\eta$  is the viscosity (c, Poise),  $T_R$  is the temperature ( $^{\circ}R$ ),  $A$  is the viscosity-temperature susceptibility curve intercept, and  $VTS$  is the slope of the relationship between viscosity and temperature susceptibility.

The transition function is developed by using viscosity-temperature susceptibility ( $VTS$ ) to divide the viscosity of the center temperature by the viscosity of each temperature, as shown in Equation (4) below [49].

$$\log(T) = c \left( 10^{A+VTS[\log(T_r)]} - 10^{A+VTS[\log(T_R)_0]} \right) \quad (4)$$

Here,  $c$  is a constant,  $T_R$  is the temperature to be converted ( $^{\circ}R$ ), and  $(T_R)_0$  is the reference temperature ( $^{\circ}R$ ).

This study performed tests based on the AASHTO TP 62 [48], which was created by the United States FHWA, to evaluate asphalt mixtures that were created using ERCRP-modified binder and normal SBS-modified binder. A super-pave gyratory compactor (SGC) was used to create test specimens with a height of 178 mm and a diameter of 150 mm. Then, core work was performed to extract final samples having a size of 150 mm  $\times$  100 mm (Figure 3A). For the dynamic modulus tests, a UTM-25 universal testing machine was used (Figure 3B). The test temperature was set from  $-10^{\circ}C$  to  $54^{\circ}C$  to understand the mixtures' physical properties at a variety of temperatures, and the loading frequency was divided into 6 levels from 25 Hz to 0.1 Hz. As in the aforementioned FST tests, a time-temperature shift factor was calculated, and the Excel program's Solver was used to fit the other elastic coefficient values horizontally based on a value of  $20^{\circ}C$ . Ultimately, the master curve was acquired with an S-shaped sigmoidal function.



**Figure 3.** (A) Specimen manufacturing process and (B) Process of measuring dynamic modulus.

### 2.3.2. Semi-Circular Bending (SCB) Test

In particular, fatigue cracking, which is one of several types of pavement damage, can quickly degrade pavement structures and drastically reduce driving quality once it occurs. Therefore, various test methods have been introduced to create mixtures that can effectively resist this kind of damage. The SCB test is similar to the indirect tensile test (IDT), which is an existing tensile failure test. Based on ASTM D8044-16 [50], the SCB tests used ERCRP-modified SBS binder and normal SBS-modified asphalt binder to fabricate the mixture. For the mixture, the tests used a normal-density 13 mm SMA that was created by the mix design process previously mentioned. For the test specimens, specimens with a diameter of 150 mm and a thickness of 50 mm were created using the gyratory compactor and cut into semi-circular shapes. Notches with a thickness of 1.5 and a length of 15 mm were added to the middle part of the specimens (Figure 4A). The tests were performed using a UTM-25 universal testing machine (Figure 4B), and the test temperature was set at  $-12\text{ }^{\circ}\text{C}$  and  $-24\text{ }^{\circ}\text{C}$  while the loading speed was set at 50 mm/min. The reaction force at the load point was monitored in real time by the data acquisition system in the UTM.

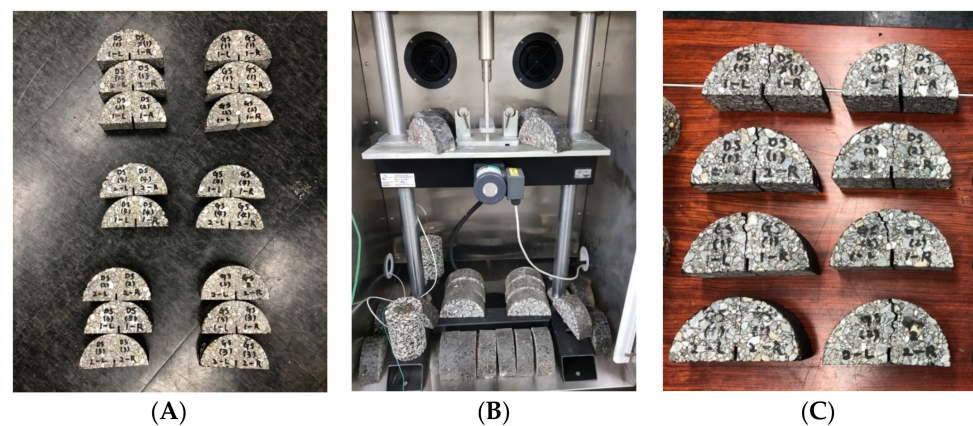


**Figure 4.** (A) SCE Specimens before testing, (B) SCB testing, and (C) Fractured specimens.

### 2.3.3. Cantabro Test

The cohesion of the asphalt binder is considered a very important element in allowing mixtures to resist damage such as potholes. As such, this study performed Cantabro tests using a Los Angeles abrasion loss tester (Figure 5A) to evaluate the aggregate shatter resistance of mixtures that use a modified binder based on the suggestion from ASTM D7064 [51] and Cox et al. [52]. In the Cantabro tests, Marshall test specimens were placed in a Los Angeles abrasion loss tester with the ball bearings removed, and the drum was rotated 30 times per minute following the KS F 2492 [53]. The mass loss ratio of the specimens after 300 rotations was used. The loss ratio was calculated using the following Equation (5) [53].

$$\text{Loss}(\%) = \frac{A - B}{A} \times 100 \quad (5)$$

Here, A: the mass of the specimen before the test (g), B: the mass of the specimen after the test (g).

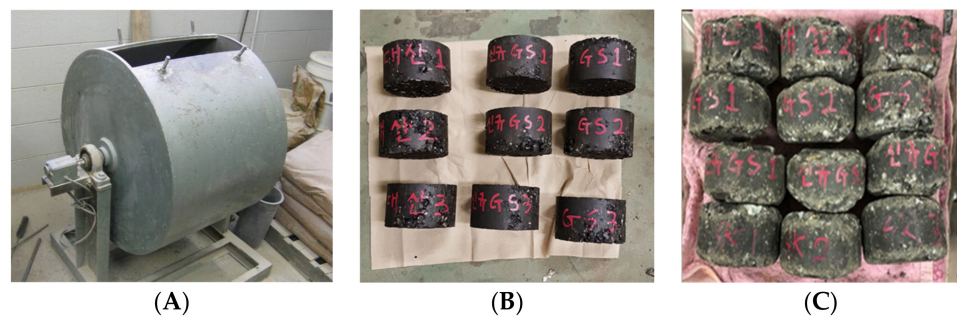


**Figure 5.** (A) Los Angeles wear loss tester; Test specimens before (B) and after (C) Cantabro test.

Generally, Cantabro is used on drainage asphalt mixtures, but it can also be used on normal mixtures. The tests were performed on 13 mm SMA Marshall test specimens using normal SBS binder, CRP modified SBS asphalt binder. Before the tests, the specimens were cured in a constant temperature chamber at 20 degrees for more than 20 h. Figure 5B,C show the specimens before and after the tests, respectively.

#### 2.4. Field Application

Asphalt pavement is gradually damaged as the service time passes and traffic loads pass through, and it requires periodic repair according to the degree of damage. Therefore, performance test results from the field testbed in the actual field are very crucial procedures to verify the effectiveness of the proposed approach. Test construction consists of sequential processes such as transportation, laying, and compaction. The testbed construction was conducted in GS Caltex Complex, a petrochemical corporation of Yeosu city, South Korea. It was constructed with a length of 50 m and a width of 10 m, as shown in Figure 6.



**Figure 6.** (A) Location of test construction in GS Caltex Complex, Yeosu city, South Korea and (B) View of test construction.

During the service period, the compaction status of the asphalt pavement was checked using non-destructive testing equipment such as LFWD (Light Falling Weight Deflectometer, hereinafter LFWD) and handy-type GPR (Ground Penetrating Radar, hereinafter GPR). The testing points of the above field experiments were conducted following Figure 7.

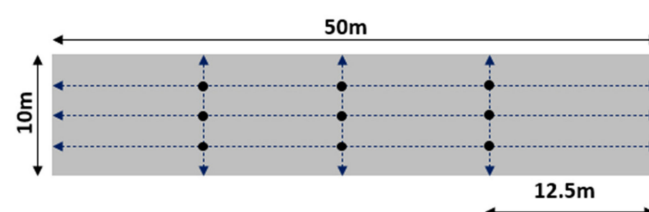


**Figure 7.** Diagram of testing point in the non-destructive testing.

#### 2.4.1. Light Falling Weight Deflectometer (LFWD) Test

In order to check the performance of the pavement after test construction, in this project, the deflection amount and modulus of elasticity of the pavement were calculated using a small impact load tester, LFWD, in accordance with ASTM 2835 [54]. The LFWD test is a miniaturized equipment of the existing FWD (Falling Weight Deflectometer, hereinafter referred to as FWD) that measures the deflection caused by the impact load of the falling weight. The basic principle is the same as the FWD test, but the test method is simple, and it is possible to test in the section where FWD cannot enter, and it has the advantage of being able to conduct the test quickly with a small number of people.

In the LFWD test, the amount of elastic settlement of the ground according to the free fall of the weight is measured with a geophone, as shown in Figure 8, and the result is converted into an elastic modulus using a data logger. Since the LFWD test calculates the modulus of elasticity by measuring the amount of elastic settlement, it is easy to modify, delete, and save data right on the test site by connecting the data logger and laptop computer or PDA with Bluetooth equipment.



**Figure 8.** On-site Light Falling Weight Deflectometer.

The measured elastic settlement is calculated as the elastic modulus value using Timoshenko's elasticity theory, which is as follows in Equation (6) [54].

$$E_{LFWD} = \frac{q_d}{w_d} \gamma \frac{\pi}{2} (1 - \nu^2) \quad (6)$$

Here,  $E_{LFWD}$ : elastic modulus calculated by LFWD,  $q_d$ : stress applied to the load plate,  $w_d$ : deflection,  $\nu$ : Poisson's ratio,  $\gamma$ : radius of the load plate.

According to the small impact load tester manual provided by Dynatest, Denmark, the modulus of recovery measured by the small impact load tester has a different range depending on the compacted material, and the general range is shown in Table 7.

**Table 7.** Range of modulus of elasticity by material according to LFWD test.

Materials	Elastic Modulus Range
Soft mud	1~20 MPa
Hard mud	20~50 MPa
Sand	30~70 MPa
Pebble	60~200 MPa

The load plate size, load weight, load height, and Poisson's ratio of the LFWD were tested by applying the conditions (see Table 8), and the FWD-Light equipment from Sokki Kenkyujo, Tokyo, Japan was used as the equipment used.

**Table 8.** LFWD field test conditions.

LFWD Test Conditions			
Diameter of the Load Plate	The Weight of the Load	Load Height	Poisson's Ratio
150 mm	15 kg	27 inch	0.4

#### 2.4.2. GPR (Ground Penetrating Radar) Exploration

GPR is an abbreviation of Ground Penetrating Radar, and it can be interpreted as radar that penetrates the ground following ASTM D4748-10 [55]. GPR survey is an electromagnetic wave survey that identifies the underground structure using electro-poration pulses in the 10 MHz to several GHz frequency band. As a result, as many constructions are recently requiring large-scale and rapid construction, and the special law on underground safety management is enacted, the utilization of underground penetrating radar exploration, such as ground investigation, is gradually increasing. The GPR survey method is a physical exploration method that obtains underground information by propagating electromagnetic waves underground in the form of short-width pulses from an antenna and then receiving and analyzing electromagnetic waves reflected from the boundary of media with different physical properties during the propagation path.

The antenna frequency used in GPR exploration is proportional to the resolution and inversely proportional to the penetrating depth. The higher the frequency, the smaller the object can be detected, but the penetration depth of the wave becomes relatively shallow. On the other hand, the lower the frequency, the deeper the penetration depth, but the lower the ability to detect objects. Therefore, the size of the object to be searched for and the expected burial depth must be sufficiently investigated in advance to select an appropriate antenna. The minimum size of a detectable object is called 'resolution,' which varies depending on the soil and refers to half the length of one wavelength. Propagation speed differs depending on each medium, and since the site is an asphalt paved road, a general average propagation speed of 110 mm/ns was applied, and 3 cases in the longitudinal direction (50 m each) and 3 cases in the lateral direction (10 m each) were applied.

### 3. Results

#### 3.1. Binder Tests

##### 3.1.1. Frequency Sweep Test

In the asphalt mixture that is normally used in road pavement, low-temperature cracking due to tensile stress mainly occurs at temperatures of 0 °C and below, and as the temperature increases to 50 °C or above, plastic deformation or permanent deformation failure modes occur more often due to shear load. This is because the asphalt binder has the properties of a typical viscoelastic material in which the elastic modulus is high at low temperatures and low at high temperatures. To predict these results, a master curve of the dynamic shear modulus was created using TTS, which is a theory in which time and temperature variables related to viscoelastic material are expressed as a single curve. FST tests were conducted on the reference and the ERCRP-modified binder by performing a series of processes, and the results are shown in Figure 9 below. In general, the FST test shows a relatively identical shape between the two mixtures. Both mixtures share the common behavior of asphalt mixture since lower temperature results in a greater shear load value. Therefore, Figure 10 was conducted to further investigate the difference in mixtures.

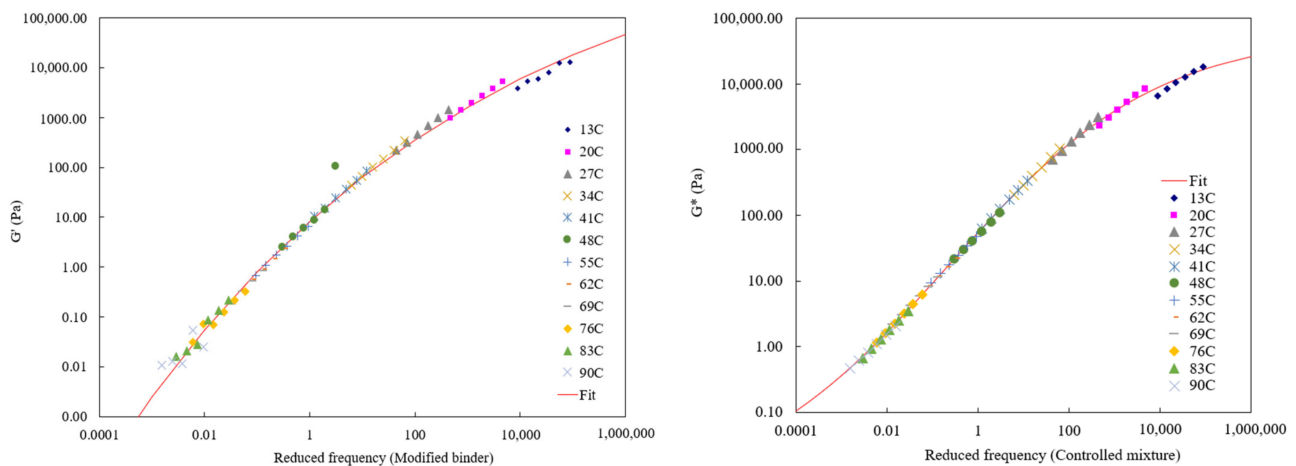


Figure 9. ERCRP-modified binder test results and controlled binder test results.

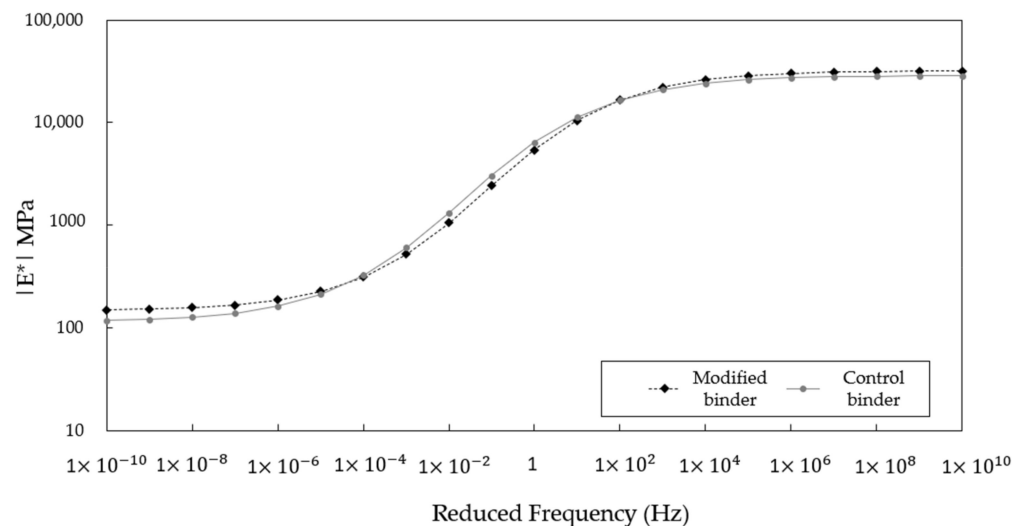


Figure 10. Dynamic modulus of test binder.

Based on the overlapping comparison of the normal SBS binder and the ERCRP-modified binder test results, although the ERCRP-modified binder slightly outperforms the control mixture at both critical stages (very slow or very high frequency), there was a neglectable performance difference concerning resistance to plastic deformation at high temperatures and resistance to temperature cracking at low temperatures.

### 3.1.2. MSCR Test

As mentioned before, the loads that were used in MSCR were 0.1 kPa and 3.2 kPa, as suggested by ASTM D7405-10a [45]. The 0.1 KPa load was applied for 1 s followed by a 9-s rest, and this process was repeated 10 times. Then, the load was increased to 3.2 kPa, and the process was repeated in the same way. In the MSCR test, the binder is exposed to increased amounts of stress and strain, thereby precisely simulating what would happen in a practical pavement. The behavior of the asphalt mixture in the MSCR test covers not only the hardening properties of the binder but also the elasticity through the use of greater degrees of stress in this test. Figure 11A,B present the MSCR test results of the modified and control SBS asphalt binder under the 0.1 and 3.2 KPa conditions, respectively. It can be seen that the cumulative strain rate due to the creep load was markedly lower in the ERCRP-modified binder than in the reference binder. In addition, the results of the comparison with the reference binders showed that the strain recovery slope of the ERCRP-modified binder was superior regardless of the creep load level. At both MSCR levels, the control binder shows a steep increase in strain while this magnitude was minor,

as shown in the modified mix. For example, at MSCR of 0.1 kPa and 190 s, the strain value of the reference and the modified mix was 38.81 and 29.43, respectively. Meanwhile, the value of MSCR 3.2 kPa and 190 s was 808.98 and 630.49 in the former and latter binders, respectively.

This confirms the modifying effect of the CRP into the asphalt binder, which may add value to the stiffness of the mix. Considering the non-recoverable compliance at a shear creep load of 3.2 kPa, the MSCR test results indicate that both binder options share the equivalent shape at an early age ranging from 100 to 120 s. However, after this stage, the accumulated strain increases significantly in the reference binder, and the longer testing time leads to a higher gap between the two binders. As a result, the findings confirm that the performance of the ERCRP-modified binder was considerably improved compared with the normal binder. The addition of CRP into the mixture not only increases the resistance to deformation but also provides elastic behavior to the binder.

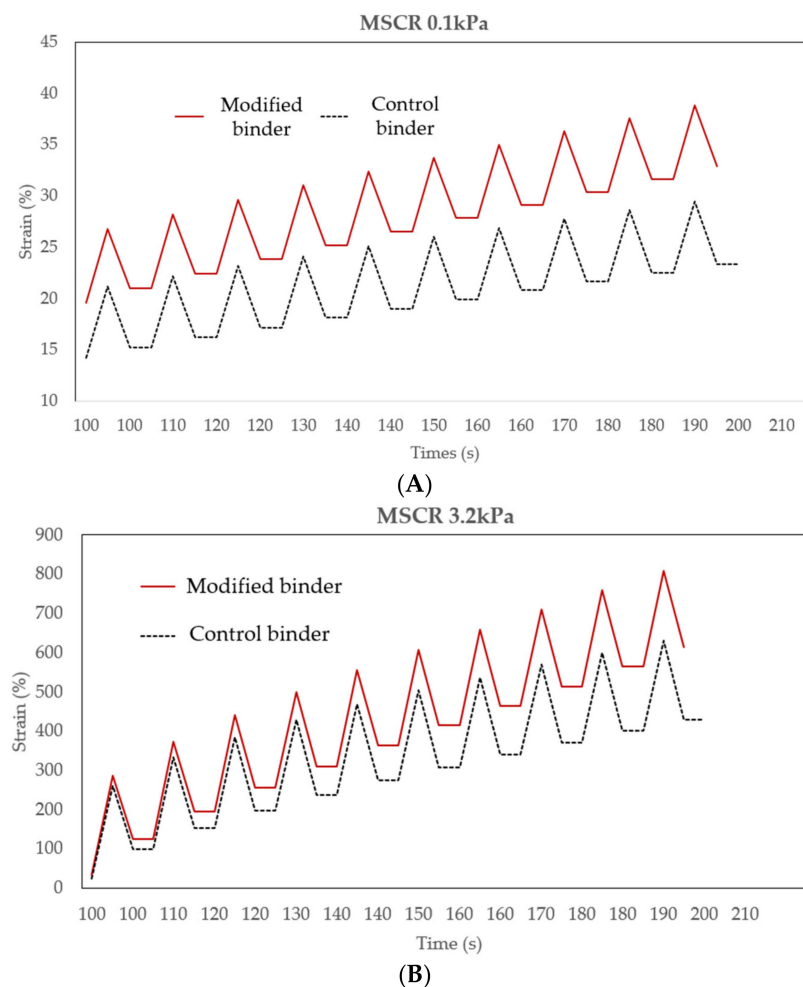


**Figure 11.** (A) MSCR test result (0.1 kPa) and (B) MSCR test result (3.2 kPa).

Additionally, the recovery (%) in Figure 12 exhibits the median elastic deformation values of the binders developed through this research. It can be observed that both SBSs mixtures show potential resistance against cracking by providing sufficient elastic recovery. The non-recovery (%) on the right side of Figure 12 indicates plastic deformation properties, and the findings notice that the modified binder had lower values than the conventional binder, suggesting a great plastic deformation.

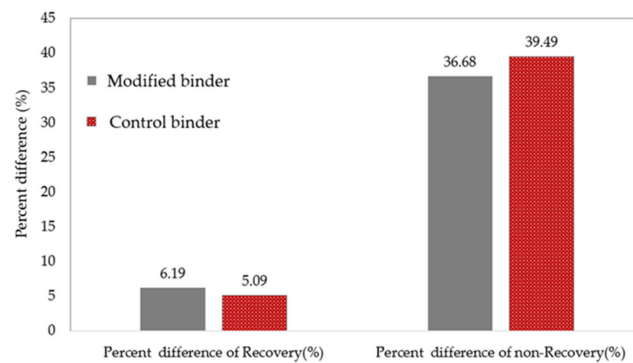


Figure 12. Recovery part (%) and non-recovery part (%).

### 3.2. Asphalt Concrete Mixture Test Results

#### 3.2.1. Dynamic Modulus Test

As depicted in Figure 13 below, the findings suggest that the ERCRP-modified and control SBS mixtures exhibited relatively similar dynamic modulus curves for all load frequencies. However, after further investigation into the critical frequency range, the ERCRP-modified specimens showed higher dynamic modulus values than the control mix in low-temperature and high-temperature regions, but they showed similar behavior in normal medium temperatures. For instance, at the highest and lowest frequency, the dynamic modulus of the ERCRP-modified samples was approximately 32,267 and 189 MPa, while the value of the reference mixture was 28,730 and 105 MPa, respectively. This can be explained by the reinforcement effect of proper CRP content into the binder, which results in the stiffening effect of the mixture and, thereby, cultivating stronger resistance under repeated loads.

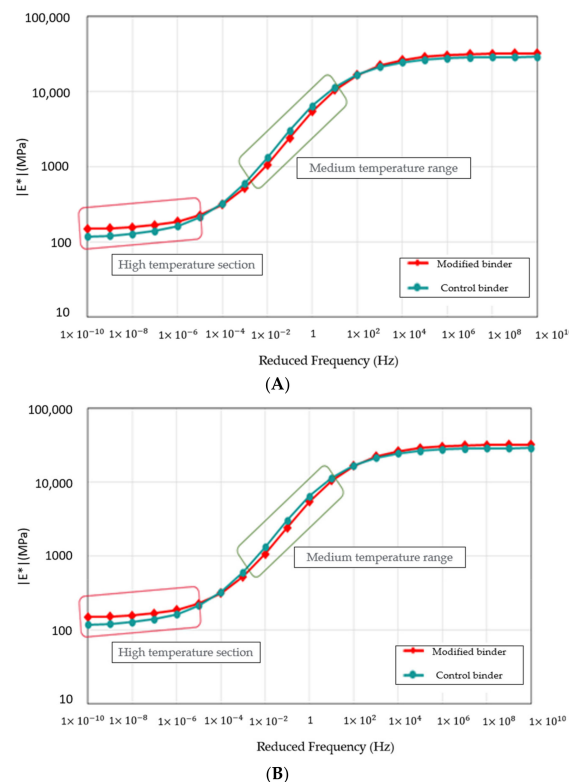
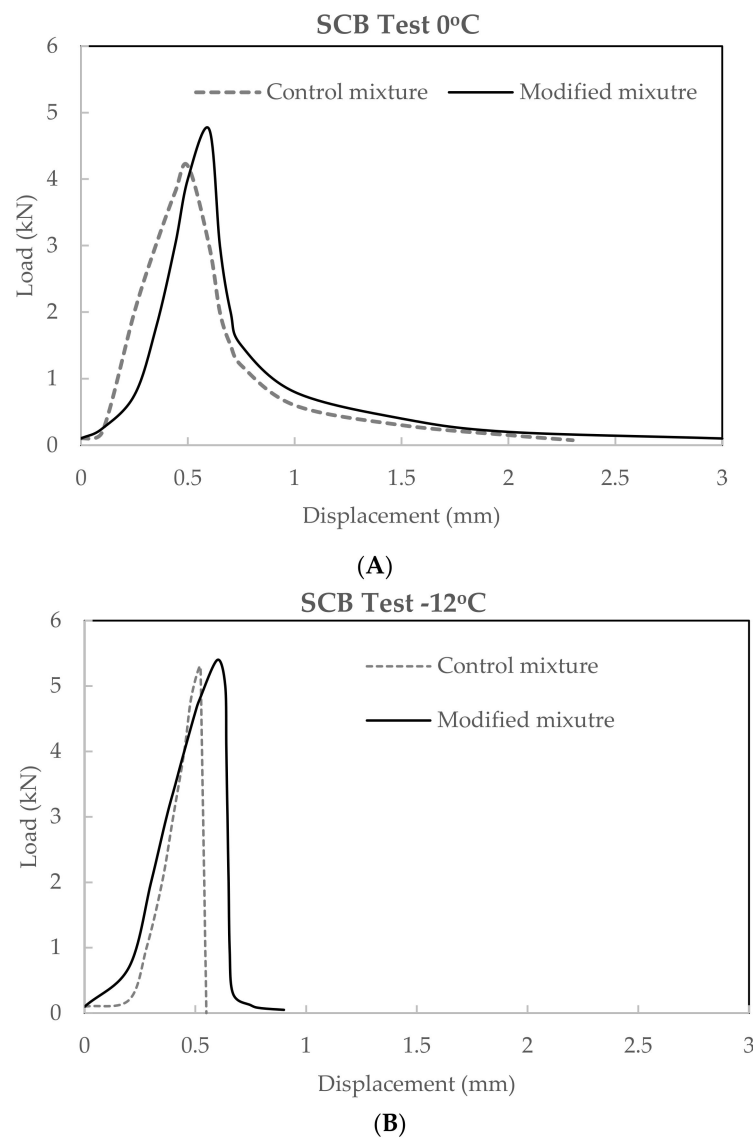


Figure 13. Master curve (HMA) of dynamic modulus test results: (A) log-log scale (high-temperature region) and (B) semi-log scale (low-temperature region).

### 3.2.2. SCB Test

Figure 14A,B demonstrate the results of SCB tests at  $-0^{\circ}\text{C}$  and  $-12^{\circ}\text{C}$ , respectively. The findings reveal that the vertical load applied to each specimen increased according to the gradual increase in displacement, which was controlled by an actuator. Once the specimens reached a fractured state at the maximum load value, the load value tended to decrease gradually until complete failure. The fracture behavior was different between testing conditions, and this is attributable to the hardened effect in the internal asphalt concrete mixture. The conditioned specimens at a lower temperature can achieve greater load, but abrupt fracture failure could be easily observed. At SCB tests conducted at  $-0^{\circ}\text{C}$  and  $-12^{\circ}\text{C}$ , the peak stress of the ERCRP-modified mixture was 4.75 and 5.4 MPa, respectively, while the value of the control mixture was only 4.2 and 5.3. Furthermore, the addition of CRP also contributes to the ductile behavior of asphalt mixture under applied load since the maximum displacement of the ERCRP-modified specimens was up to 3 mm. Meanwhile, the conventional samples can only reach 2.5 mm.



**Figure 14.** SCB test results (A) at  $0^{\circ}\text{C}$  and (B) at  $-12^{\circ}\text{C}$ .

Table 9 below shows the fracture energy for each specimen. Fracture energy is a failure property that is used to evaluate resistance to cracking in asphalt mixtures, and it refers to the total energy that is applied to the specimen until the specimen fails. In the test results, the ERCRP-modified specimens had a superior fracture energy value of  $820 \text{ J/m}^2$  at  $-0 \text{ }^\circ\text{C}$ , which was 8% higher than that of the reference specimens ( $766 \text{ J/m}^2$ ), indicating this mixture also acquires a higher resistance for practical application in cold regions. Considering the conditioning at  $-12 \text{ }^\circ\text{C}$ , the average fracture energy was  $518 \text{ J/m}^2$ , which was 23.75% larger than that of the control specimen.

**Table 9.** Average fracture energy ( $-12 \text{ }^\circ\text{C}$ ) and average fracture energy ( $-24 \text{ }^\circ\text{C}$ ).

Mix	$0 \text{ }^\circ\text{C}$ Fracture Energy ( $\text{J/m}^2$ )	Mix	$-12 \text{ }^\circ\text{C}$ Fracture Energy ( $\text{J/m}^2$ )
Control	766	Control	395
Modified	820	Modified	518

Table 9 also shows the rate of change in fracture energy according to temperature. The findings suggest that the ERCRP-modified specimen was the least affected by temperature, which suffered from a drop of about 36% in fracture energy. On the other hand, the controlled specimen showed lower values than the ERCRP-modified specimen, with degradation of more than 48%.

Based on the experiment results, it was determined that the mixture using the ERCRP-modified binder obtained feasible resistance against cracking. Due to the modification effect of using the proper content of CRP, it is expected to exhibit resilient characteristics and develop cracks gradually rather than fracturing suddenly.

### 3.2.3. Cantabro Durability Test

The Cantabro test results are summarized in Table 10. The original specimen weight was referred to as the dry weight of each Marshall test specimen, while the weight after testing was the final weight of the specimen subjecting to the tester 300 times at 30 times per minute. Overall, the Cantabro process caused critical surface damage to the test specimens, and the damage ratios (%) can be easily observed among all conditions.

**Table 10.** Summary of Cantabro test.

	Specimen Weight (g)	Weight after the Test (g)	Loss Rate (within 20% Based on Drainage)	Average Loss Rate (%)
Controlled mix 1	1191.0	1045.8	12.191	
Controlled mix 2	1193.4	1017.3	14.756	12.192
Controlled mix 3	1192.4	1077.6	9.628	
ERCRP-modified mix 1	1193.3	1112.4	6.780	
ERCRP-modified mix 2	1192.3	1033.0	13.361	10.375
ERCRP-modified mix 3	1193.4	1112.4	10.985	

Based on the test results, the ERCRP-modified specimen showed a loss rate of 10.375%, which was an improvement over the normal specimen, which had a loss rate of 12.192%. The improvement in effectiveness may be explained by the stiffening effect contributed by the incorporation of CRP. This finding confirms the results from the above dynamic modulus and SCB test, which indicate the ductile behavior of ERCRP-modified mixtures as well as the stronger bearing capacity.

### 3.3. Field Test Results

#### 3.3.1. LFWD Test Results

Table 11 presents the LFWD test results between ERCRP-modified pavement and control pavement. In general, the applied falling weight leads to the average pavement maximum loads of 4464 and 4151 N in the former and latter options. Although ERCRP-modified pavement received greater maximum loads compared with the control one, the maximum displacement among them showed comparable results, with the maximum displacement value ranging from 0.1 to 0.11 mm, respectively. As a result of the measured elastic modulus from a field test, the FLWD showed a slight improvement (6.75%) in the reinforcement effectiveness when using the CRP as a binder modifier in SBS pavements. This finding suggests that usage of CRP not only reduces the asphalt binder cost but also promotes the utilization of by-product materials in practice and thereby contributing to the development of sustainable pavements.

**Table 11.** LFWD test results.

No.	Maximum Load (N)		Maximum Displacement (mm)		Elastic Modulus (MPa)	
	ERCRP-Modified Pavement	Controlled Pavement	ERCRP-Modified Pavement	Controlled Pavement	ERCRP-Modified Pavement	Controlled Pavement
1	4649	4327	0.151	0.163	35.7	32.8
2	4495	4185	0.097	0.105	53.7	48.7
3	4470	4159	0.096	0.1	53.9	50.6
4	4466	4155	0.117	0.129	44.2	43.1
5	4454	4148	0.084	0.085	61.4	55.9
6	4478	4169	0.077	0.089	57.4	53.5
7	4370	4061	0.107	0.115	47.3	44.6
8	4417	4102	0.093	0.097	55	52.5
9	4376	4065	0.103	0.112	49.2	45.2
Average	4464	4152	0.1	0.11	50.87	47.43

#### 3.3.2. GPR Test Results

As a result of GPR surveys conducted to investigate the overall construction condition (see Figure 15), the pavement thickness of the asphalt layer was generally uniform at around 0.25 m from the top of the pavement. In other words, the gap of GPR illustration lines from the top indication to the depth of 0.25 m was very consistent. Overall, both pavements showed homogeneous distribution of asphalt along the testing site, and there was no sign of a failure point in the surface layer. Hence, the test confirms the applicability of ER and CRP in modified SBS asphalt concrete mixture for actual construction. However, further long-term monitoring works should be conducted to verify the durability of pavement after prolonged traffic service life. In addition, the next stage of this research will focus on the cost-effectiveness of the proposed approach to promote this for large-scale applications.

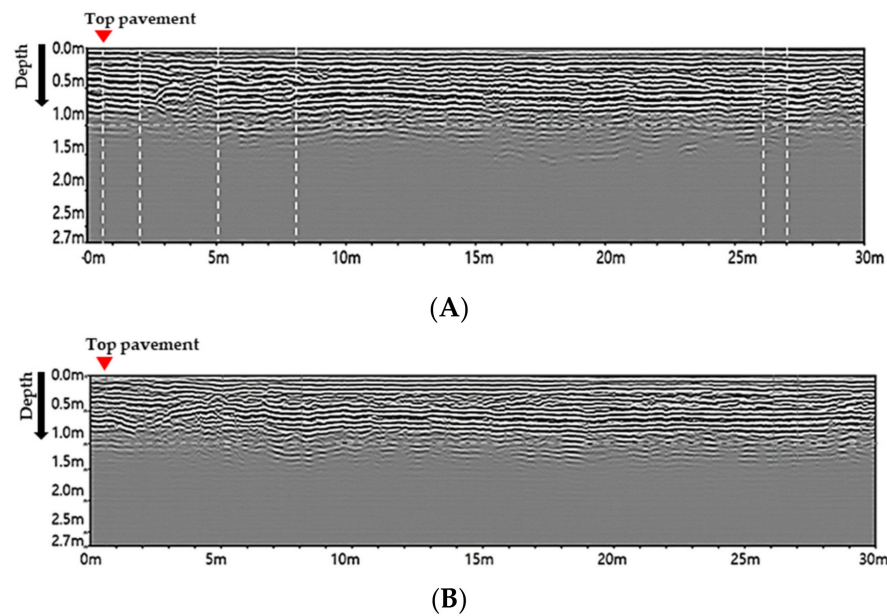


**Figure 15.** Sectional image of GPR exploration results. (A) Modified Sections. (B) Controlled Sections.

#### 4. Conclusions

The proposed research aimed to incorporate epoxy resin (ER) and crumb rubber powder (CRP) contents to reduce the consumption of conventional asphalt binder and also promote the usage of recycled waste rubber in practice. To cope with this research objective, the ER and CRP were designed at 3% and 5% by weight of asphalt binder, respectively. In this research, various laboratory tests were performed to evaluate the rheological properties of modified asphalt binders as well as the performance of the proposed asphalt concrete mix, including Frequency Sweep Test, Multiple Stressed Creep and Recovery, Dynamic Modulus, Semi Circular Bending, Cantabro Durability Tests. Afterward, to verify the practical application of the newly developed material, a long-term performance review via field testbed was performed containing Falling Weight Deflectometer and Ground Penetrating Radar tests. The following conclusions can be drawn from the research:

- As a result of the frequency sweep test, the high-temperature plastic deformation resistance and low-temperature crack resistance showed almost similar results between the ER/CRP-modified and reference mixtures.
- However, the improvement of ER and CRP in the ER/CRP-modified binder was vital when the creep test was taken into account. The MSCR test result indicates that the cumulative strain of the ER/CRP-modified binder due to creep load was significantly reduced compared with the reference mix. For instance, at MSCR of 0.1 kPa and 190 s, the strain value of the modified and reference mix was 29.43 and 38.81, respectively. On the other hand, the value of MSCR 3.2 kPa and 190 s was 630.49 and 808.98 in the former and latter binders, respectively. This confirms the contribution of the CRP to the deformation resistivity of the asphalt binder.
- In addition, the recovery (%) in the MSCR test also shows that both SBSs mixtures show potential resistance against cracking by providing sufficient elastic recovery. The plastic deformation (%) of the ER/CRP-modified binder was lower than the conventional binder, suggesting a great plastic deformation resistance.
- Considering the behavior of asphalt concrete mixture at the critical frequency loads, the ER/CRP-modified specimens obtained higher dynamic modulus values than the control mix in both low-temperature and high-temperature regions. For example, the dynamic modulus of the ER/CRP-modified samples was approximately 32,267 and 189 MPa, while the value of the reference mixture was 28,730 and 105 MPa at the highest and lowest frequency, respectively.

- Regarding the SCB test results at  $-0\text{ }^{\circ}\text{C}$  and  $-12\text{ }^{\circ}\text{C}$ , the peak stress of the ERCRP-modified mixture was 4.75 and 5.4 MPa, respectively, while the value of the reference specimens was only 4.2 and 5.3 MPa, noticing the slight stress-bearing capacity improvement. Furthermore, the addition of CRP also enhances the ductile behavior of asphalt mixture under applied load since the maximum displacement of the ERCRP-modified specimens was up to 3 mm while this value of the conventional samples was 2.5 mm.
- Based on the test durability test results, the ERCRP-modified mix and reference samples present a loss rate of 10.375% and 12.192%, respectively, indicating a slight improvement in the durability of the modified mixture.
- Through in full-scale testbed, the FLWD elastic modulus of reinforced pavement shows a slight improvement (6.75%) compared with the control pavement. In general, based on the laboratory and field tests, the results confirm that usage of ERCRP not only diminishes the consumption of conventional asphalt binder but also promotes the utilization of by-product materials in practice and thereby developing the sustainable infrastructure objective.

**Author Contributions:** S.-Y.L., T.H.M.L.: conceptualization, methodology, writing—original draft. S.-Y.L. and T.H.M.L.: visualization, investigation, writing—review and editing. S.-Y.L. and T.H.M.L.: data curation, software. All authors have read and agreed to the published version of the manuscript.

**Funding:** Korea Ministry of SMEs and Startups.

**Institutional Review Board Statement:** Not applicable.

**Informed Consent Statement:** Not applicable.

**Data Availability Statement:** Data will be provided on request.

**Acknowledgments:** Research for this paper was carried out under the Korea Technology and Information Promotion Agency for SMEs Research Program (project no. S3044598, Research on development of large-scale utilization technology of waste plastic through road system multi application) funded by the Ministry of SMEs and Startups.

**Conflicts of Interest:** The authors declare no conflict of interest, financial or otherwise.

## References

1. Yang, T.; Jia, Y.; Pan, Y.; Zhao, Y. Evaluation of the Low-Temperature Cracking Performance of Recycled Asphalt Mixture: A Development of Equivalent Fracture Temperature. *Buildings* **2022**, *12*, 1366. [\[CrossRef\]](#)
2. Wang, Y.; Lin, G.; Li, Z. Dynamic Response of Anisotropic Multilayered Road Structures Induced by Moving Loads Based on a Novel Spectral Element Method. *Buildings* **2022**, *12*, 1354. [\[CrossRef\]](#)
3. Li, M.; Luo, C.; Zhu, L.; Li, H.; Cong, P.; Feng, Y.; Yan, L. A novel epoxy-terminated polyethylene modified asphalt with low-viscosity and high storage stability. *Constr. Build. Mater.* **2022**, *335*, 127473. [\[CrossRef\]](#)
4. Huang, G.; Yang, T.; He, Z.; Yu, L.; Xiao, H. Polyurethane as a modifier for road asphalt: A literature review. *Constr. Build. Mater.* **2022**, *356*, 129058. [\[CrossRef\]](#)
5. Li, Y.; Chai, J.; Wang, R.; Zhou, Y.; Tong, X. A Review of the Durability-Related Features of Waste Tyre Rubber as a Partial Substitute for Natural Aggregate in Concrete. *Buildings* **2022**, *12*, 1975. [\[CrossRef\]](#)
6. Fan, Y.; Wu, Y.; Chen, H.; Liu, S.; Huang, W.; Wang, H.; Yang, J. Performance Evaluation and Structure Optimization of Low-Emission Mixed Epoxy Asphalt Pavement. *Materials* **2022**, *15*, 6472. [\[CrossRef\]](#)
7. Pstrowska, K.; Gunka, V.; Prysiazny, Y.; Demchuk, Y.; Hrynychuk, Y.; Sidun, I.; Kułazyński, M.; Bratychak, M. Obtaining of Formaldehyde Modified Tars and Road Materials on Their Basis. *Materials* **2022**, *15*, 5693. [\[CrossRef\]](#)
8. Gamage, S.; Palitha, S.; Meddage, D.P.P.; Mendis, S.; Azamathulla, H.M.; Rathnayake, U. Influence of Crumb Rubber and Coconut Coir on Strength and Durability Characteristics of Interlocking Paving Blocks. *Buildings* **2022**, *12*, 1001. [\[CrossRef\]](#)
9. Guo, L.; Xu, W.; Zhang, Y.; Ji, W.; Wu, S. Selecting the Best Performing Modified Asphalt Based on Rheological Properties and Microscopic Analysis of RPP/SBS Modified Asphalt. *Materials* **2022**, *15*, 8616. [\[CrossRef\]](#)
10. Cui, S.; Guo, N.; Wang, L.; You, Z.; Tan, Y.; Guo, Z.; Luo, X.; Chen, Z. Effect of Freeze–Thaw cycles on the pavement performance of SBS modified and composite crumb rubber modified asphalt mixtures. *Constr. Build. Mater.* **2022**, *342*, 127799. [\[CrossRef\]](#)
11. Li, Y.; Yan, X.; Guo, J.; Wu, W.; Shi, W.; Xu, Q.; Ji, Z. Performance and Verification of High-Modulus Asphalt Modified by Styrene-Butadiene-Styrene Block Copolymer (SBS) and Rock Asphalt. *Coatings* **2022**, *13*, 38. [\[CrossRef\]](#)

12. Li, H.; Cui, C.; Temitope, A.A.; Feng, Z.; Zhao, G.; Guo, P. Effect of SBS and crumb rubber on asphalt modification: A review of the properties and practical application. *J. Traffic Transp. Eng.* **2022**, *9*, 836–863. [\[CrossRef\]](#)
13. Ma, Y.; Wang, S.; Zhang, M.; Jiang, X.; Polaczyk, P.; Huang, B. Weather aging effects on modified asphalt with rubber-polyethylene composites. *Sci. Total. Environ.* **2023**, *865*, 161089. [\[CrossRef\]](#)
14. Poulidakos, L.D.; Pasquini, E.; Tusar, M.; Hernando, D.; Wang, D.; Mikhailenko, P.; Pasetto, M.; Baliello, A.; Falchetto, A.C.; Miljković, M.; et al. RILEM interlaboratory study on the mechanical properties of asphalt mixtures modified with polyethylene waste. *J. Clean. Prod.* **2022**, *375*, 134124. [\[CrossRef\]](#)
15. Davoodi, A.; Esfahani, M.A.; Bayat, M.; Mohammadyan-Yasouj, S.E.; Rahman, A. Influence of nano-silica modified rubber mortar and EVA modified porous asphalt on the performance improvement of modified semi-flexible pavement. *Constr. Build. Mater.* **2022**, *337*, 127573. [\[CrossRef\]](#)
16. Chen, R.; Zhao, R.; Liu, Y.; Xi, Z.; Cai, J.; Zhang, J.; Wang, Q.; Xie, H. Development of eco-friendly fire-retarded warm-mix epoxy asphalt binders using reactive polymeric flame retardants for road tunnel pavements. *Constr. Build. Mater.* **2021**, *284*, 122752. [\[CrossRef\]](#)
17. Han, X.; Mao, S.; Zeng, S.; Duan, H.; Liu, Q.; Xue, L.; Yu, J. Effect of reactive flexible rejuvenators on thermal-oxidative aging resistance of regenerated SBS modified asphalt. *J. Clean. Prod.* **2022**, *380*, 135027. [\[CrossRef\]](#)
18. Zhang, Z.; Li, J.; Wang, Z.; Long, S.; Jiang, S.; Liu, G. Preparation and performance characterization of a novel high-performance epoxy resin modified reactive liquid asphalt. *Constr. Build. Mater.* **2020**, *263*, 120113. [\[CrossRef\]](#)
19. Saputra, R.; Walvekar, R.; Khalid, M.; Mubarak, N.M.; Sillanpää, M. Current progress in waste tire rubber devulcanization. *Chemosphere* **2021**, *265*, 129033. [\[CrossRef\]](#)
20. Boucher, J.; Friot, D. Primary Microplastics in the Oceans. *Mar. Environ. Res.* **2017**, *111*, 18–26.
21. Akbas, A.; Yuhana, N.Y. Recycling of Rubber Wastes as Fuel and Its Additives. *Recycling* **2021**, *6*, 78. [\[CrossRef\]](#)
22. Zheng, W.; Wang, H.; Chen, Y.; Ji, J.; You, Z.; Zhang, Y. A review on compatibility between crumb rubber and asphalt binder. *Constr. Build. Mater.* **2021**, *297*, 123820. [\[CrossRef\]](#)
23. Memon, N.A. Comparison between Superpave Gyrotory and Marshall Laboratory Compaction Methods. Doctoral Dissertation, Universiti Teknologi Malaysia, Skudai, Malaysia, 2006.
24. ASTM C127; Standard Test Method for Density, Relative Density (Specific Gravity), and Absorption of Coarse Aggregate. Annual Book of ASTM Standard. ASTM International: West Conshohocken, PA, USA, 2004; pp. 1–5.
25. ASTM Standard D5821; Standard Test Method for Determining the Percentage of Fractured Particles in Coarse Aggregate. ASTM International: West Conshohocken, PA, USA, 2017; pp. 1–6.
26. ASTM C131/C131M-14; Standard Test Method for Resistance to Degradation of Small-Size Coarse Aggregate by Abrasion and Impact in the Los Angeles Machine; Annual Book of ASTM Standard. ASTM International: West Conshohocken, PA, USA, 2014; Volume 4, pp. 5–8.
27. ASTM D 4791; Flat Particles, Elongated Particles, or Flat and Elongated Particles in Coarse Aggregate. ASTM International: West Conshohocken, PA, USA, 1999; Volume 4, pp. 1–4.
28. ASTM D24; Standard Specification for Mineral Filler For Bituminous Paving Mixtures. ASTM International: West Conshohocken, PA, USA, 2001; Volume 4, pp. 1–2.
29. Gao, J.; Yao, Y.; Huang, J.; Yang, J.; Song, L.; Xu, J.; Lu, X. Effect of Hot Mixing Duration on Blending, Performance, and Environmental Impact of Central Plant Recycled Asphalt Mixture. *Buildings* **2022**, *12*, 1057. [\[CrossRef\]](#)
30. Cong, P.; Luo, W.; Xu, P.; Zhang, Y. Chemical and physical properties of hot mixing epoxy asphalt binders. *Constr. Build. Mater.* **2019**, *198*, 1–9. [\[CrossRef\]](#)
31. Zhang, H.; Zhang, Y.; Chen, J.; Liu, W.; Wang, W. Effect of Desulfurization Process Variables on the Properties of Crumb Rubber Modified Asphalt. *Polymers* **2022**, *14*, 1365. [\[CrossRef\]](#)
32. Ghafari, S.; Ranjbar, S.; Ehsani, M.; Nejad, F.M.; Paul, P. Sustainable crumb rubber modified asphalt mixtures based on low-temperature crack propagation characteristics using the response surface methodology. *Theor. Appl. Fract. Mech.* **2023**, *123*, 103718. [\[CrossRef\]](#)
33. ASTM D5; Standard Test Method for Penetration of Bituminous Materials. ASTM International: West Conshohocken, PA, USA, 2019.
34. ASTM D36-16; Standard Test Method for Softening Point of Bitumen (Ring-and-Ball Apparatus). ASTM International: West Conshohocken, PA, USA, 2016.
35. ASTM D113-17; Standard Test Method for Ductility of Asphalt Materials. ASTM International: West Conshohocken, PA, USA, 2017.
36. ASTM D2872-22; Standard Test Method for Effect of Heat and Air on a Moving Film of Asphalt (Rolling Rolling Thin-Film Oven Test) Annual Book of ASTM Standard. ASTM International: West Conshohocken, PA, USA, 2022; pp. 1–6.
37. AASHTO R 28-09; Accelerated Aging of Asphalt Binder Using a Pressurized Aging Vessel (PAV). Canadian Council of Independent Laboratories: Burlington, ON, USA, 2007; pp. 1–8.
38. T313-10 A; Determining the Flexural Creep Stiffness of Asphalt Binder Using the Bending Beam Rheometer (BBR). AASHTO: Washington, DC, USA, 2011; Standard Specifications for Transportation Materials and Methods of Sampling and Testing. pp. 1–21.
39. Cho, Y.-H.; Yun, T.; Kim, I.T.; Choi, N.R. The application of Recycled Concrete Aggregate (RCA) for Hot Mix Asphalt (HMA) base layer aggregate. *KSCE J. Civ. Eng.* **2011**, *15*, 473–478. [\[CrossRef\]](#)
40. ASTM D7552-22; Standard Test Method for Determining the Complex Shear Modulus ( $G^*$ ) of Bituminous Mixtures Using Dynamic Shear Rheometer. ASTM International: West Conshohocken, PA, USA, 2016; Volume I, pp. 1–11.

41. Lee, H.J.; Lee, J.H.; Park, H.M. Performance evaluation of high modulus asphalt mixtures for long life asphalt pavements. *Constr. Build. Mater.* **2007**, *21*, 1079–1087. [[CrossRef](#)]
42. Saboo, N.; Mudgal, A.; Singh, A. Using Frequency Sweep Test to Predict Creep and Recovery Response of Asphalt Binders. *J. Mater. Civ. Eng.* **2019**, *31*, 04019081. [[CrossRef](#)]
43. Walubita, L.F.; Alvarez, A.E.; Simate, G.S. Evaluating and comparing different methods and models for generating relaxation modulus master-curves for asphalt mixes. *Constr. Build. Mater.* **2011**, *25*, 2619–2626. [[CrossRef](#)]
44. Zhang, X.; Han, C.; Yang, J.; Xu, X.; Zhang, F. Evaluating the Rheological Properties of High-Modulus Asphalt Binders Modified with Rubber Polymer Composite Modifier. *Materials* **2021**, *14*, 7727. [[CrossRef](#)] [[PubMed](#)]
45. *ASTM D7405*; Standard Test Method for Multiple Stress Creep and Recovery (MSCR) of Asphalt Binder Using a Dynamic Shear Rheometer. ASTM International: West Conshohocken, PA, USA, 2020; pp. 1–4.
46. *AASHTO T 350*; Standard Method of Test for Multiple Stress Creep Recovery (MSCR) Test of Asphalt Binder Using a Dynamic Shear Rheometer (DSR). AASHTO: Washington, DC, USA, 2009; Volume 3, pp. 1–9.
47. *ASTM D6373-21a*; Standard Specification for Performance-Graded Asphalt Binder. ASTM International: West Conshohocken, PA, USA, 2021.
48. *AASHTO TP62-2017*; Standard Method of Test for Determining Dynamic Modulus of Hot Mix Asphalt (HMA). AASHTO: Washington, DC, USA, 2017.
49. Lee, K.; Kim, H.; Kim, N.; Kim, Y. Dynamic Modulus of Asphalt Mixtures for Development of Korean Pavement Design Guide. *J. Test. Eval.* **2007**, *35*, 143–150. [[CrossRef](#)]
50. *ASTM D8044-16*; Standard Test Method for Evaluation of Asphalt Mixture Cracking Resistance Using the Semi-Circular Bend Test (SCB) at Intermediate Temperatures. ASTM International: West Conshohocken, PA, USA, 2016; pp. 1–7.
51. *ASTM D 7064-08*; Standard Practice for Open-Graded Friction Course (OGFC) Mix Design. ASTM International: West Conshohocken, PA, USA, 2013; Volume 8, pp. 1–7.
52. Cox, B.C.; Smith, B.T.; Howard, I.L.; James, R.S. State of Knowledge for Cantabro Testing of Dense Graded Asphalt. *J. Mater. Civ. Eng.* **2017**, *29*, 0002020. [[CrossRef](#)]
53. *KS F 2492*; Cantabro Test Method for Drainage Asphalt Mixtures. Korean Standard: Seoul, Republic of Korea, 2017.
54. *ASTM E2835-07*; Standard Test Method for Measuring Deflections with a Light Weight Deflectometer (LWD). ASTM International: West Conshohocken, PA, USA, 2015; Volume 7, pp. 5–7.
55. *ASTM D4748-10*; Standard Test Method for Determining the Thickness of Bound Pavement Layers Using Short-Pulse Radar. Annual Book of ASTM Standard. ASTM International: West Conshohocken, PA, USA, 1998; Volume 10, p. 7.

**Disclaimer/Publisher’s Note:** The statements, opinions and data contained in all publications are solely those of the individual author(s) and contributor(s) and not of MDPI and/or the editor(s). MDPI and/or the editor(s) disclaim responsibility for any injury to people or property resulting from any ideas, methods, instructions or products referred to in the content.